

Today's Outline - October 24, 2016

Today's Outline - October 24, 2016

- Modulated structures

Today's Outline - October 24, 2016

- Modulated structures
- Lattice vibrations

Today's Outline - October 24, 2016

- Modulated structures
- Lattice vibrations
- Powder diffraction

Today's Outline - October 24, 2016

- Modulated structures
- Lattice vibrations
- Powder diffraction
- Bragg & Laue geometries

Today's Outline - October 24, 2016

- Modulated structures
- Lattice vibrations
- Powder diffraction
- Bragg & Laue geometries
- Reflection for a Single Layer

Today's Outline - October 24, 2016

- Modulated structures
- Lattice vibrations
- Powder diffraction
- Bragg & Laue geometries
- Reflection for a Single Layer
- Kinematical Approach for Many Layers

Today's Outline - October 24, 2016

- Modulated structures
- Lattice vibrations
- Powder diffraction
- Bragg & Laue geometries
- Reflection for a Single Layer
- Kinematical Approach for Many Layers
- Darwin Curve

Today's Outline - October 24, 2016

- Modulated structures
- Lattice vibrations
- Powder diffraction
- Bragg & Laue geometries
- Reflection for a Single Layer
- Kinematical Approach for Many Layers
- Darwin Curve
- Dynamical Diffraction Theory

Today's Outline - October 24, 2016

- Modulated structures
- Lattice vibrations
- Powder diffraction
- Bragg & Laue geometries
- Reflection for a Single Layer
- Kinematical Approach for Many Layers
- Darwin Curve
- Dynamical Diffraction Theory

Homework Assignment #05:

Chapter 5: 1, 3, 7, 9, 10

due Wednesday, November 02, 2016

Today's Outline - October 24, 2016

- Modulated structures
- Lattice vibrations
- Powder diffraction
- Bragg & Laue geometries
- Reflection for a Single Layer
- Kinematical Approach for Many Layers
- Darwin Curve
- Dynamical Diffraction Theory

Homework Assignment #05:

Chapter 5: 1, 3, 7, 9, 10

due Wednesday, November 02, 2016

No class on Wednesday, November 9, 2016

Modulated structures

By definition crystals have always been considered to have long range order.



Modulated structures

By definition crystals have always been considered to have long range order.

However, it is common to see structures where the positions of the atoms is modulated (e.g. charge density waves, magnetic lattices, etc.) according to $x_n = an + u \cos(qan)$, where: a is the lattice parameter, u is the amplitude of the displacement, and $q = 2\pi/\lambda_m$ is the wave vector of the modulation.

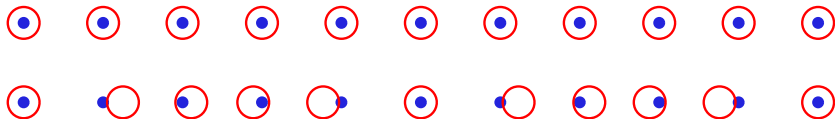


Modulated structures

By definition crystals have always been considered to have long range order.

However, it is common to see structures where the positions of the atoms is modulated (e.g. charge density waves, magnetic lattices, etc.) according to $x_n = an + u \cos(qan)$, where: a is the lattice parameter, u is the amplitude of the displacement, and $q = 2\pi/\lambda_m$ is the wave vector of the modulation.

If λ_m is a multiple or a rational fraction of a , it is called a **commensurate** modulation

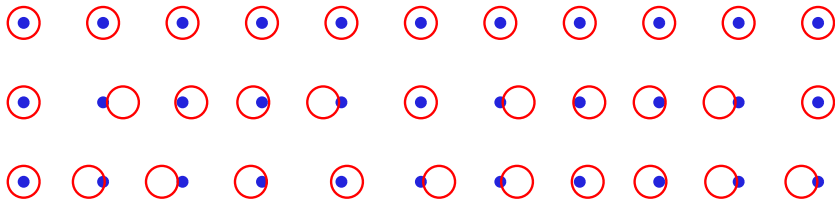


Modulated structures

By definition crystals have always been considered to have long range order.

However, it is common to see structures where the positions of the atoms is modulated (e.g. charge density waves, magnetic lattices, etc.) according to $x_n = an + u \cos(qan)$, where: a is the lattice parameter, u is the amplitude of the displacement, and $q = 2\pi/\lambda_m$ is the wave vector of the modulation.

If λ_m is a multiple or a rational fraction of a , it is called a **commensurate** modulation but if $\lambda_m = ca$, where c is an irrational number, then it is an **incommensurate** modulation.



Diffraction from a modulation

For simple a 1D modulated structure, we can compute the scattering

Diffraction from a modulation

For simple a 1D modulated structure, we can compute the scattering

$$A(Q) = \sum_{n=0}^{N-1} e^{iQx_n}$$

Diffraction from a modulation

For simple a 1D modulated structure, we can compute the scattering assuming

$$x_n = an + u \cos(qan)$$

and that the scattering factor for each atom is set to unity

$$A(Q) = \sum_{n=0}^{N-1} e^{iQx_n}$$

Diffraction from a modulation

For simple a 1D modulated structure, we can compute the scattering assuming

$$x_n = an + u \cos(qan)$$

and that the scattering factor for each atom is set to unity

$$A(Q) = \sum_{n=0}^{N-1} e^{iQx_n} = \sum_{n=0}^{N-1} e^{iQ(an + \cos(qan))}$$

Diffraction from a modulation

For simple a 1D modulated structure, we can compute the scattering assuming

$$x_n = an + u \cos(qan)$$

and that the scattering factor for each atom is set to unity

$$\begin{aligned} A(Q) &= \sum_{n=0}^{N-1} e^{iQx_n} = \sum_{n=0}^{N-1} e^{iQ(an + \cos(qan))} \\ &= \sum_{n=0}^{N-1} e^{iQan} e^{iQu \cos(qan)} \end{aligned}$$

Diffraction from a modulation

For simple a 1D modulated structure, we can compute the scattering assuming

$$x_n = an + u \cos(qan)$$

and that the scattering factor for each atom is set to unity

for the displacement u small, this becomes

$$\begin{aligned} A(Q) &= \sum_{n=0}^{N-1} e^{iQx_n} = \sum_{n=0}^{N-1} e^{iQ(an + \cos(qan)u)} \\ &= \sum_{n=0}^{N-1} e^{iQan} e^{iQu \cos(qan)} \end{aligned}$$

Diffraction from a modulation

For simple a 1D modulated structure, we can compute the scattering assuming

$$x_n = an + u \cos(qan)$$

and that the scattering factor for each atom is set to unity

for the displacement u small, this becomes

$$\begin{aligned} A(Q) &= \sum_{n=0}^{N-1} e^{iQx_n} = \sum_{n=0}^{N-1} e^{iQ(an + \cos(qan))} \\ &= \sum_{n=0}^{N-1} e^{iQan} e^{iQu \cos(qan)} \\ A(Q) &\approx \sum_{n=0}^{N-1} e^{iQan} [1 + iQu \cos(qan) + \dots] \end{aligned}$$

Diffraction from a modulation

For simple a 1D modulated structure, we can compute the scattering assuming

$$x_n = an + u \cos(qan)$$

and that the scattering factor for each atom is set to unity

for the displacement u small, this becomes

$$A(Q) \approx \sum_{n=0}^{N-1} e^{iQan} + i \left(\frac{Qu}{2} \right) \left[e^{i(Q+q)an} + e^{-i(Q-q)an} \right]$$

$$A(Q) = \sum_{n=0}^{N-1} e^{iQx_n} = \sum_{n=0}^{N-1} e^{iQ(an + \cos(qan))}$$

$$= \sum_{n=0}^{N-1} e^{iQan} e^{iQu \cos(qan)}$$

$$A(Q) \approx \sum_{n=0}^{N-1} e^{iQan} [1 + iQu \cos(qan) + \dots]$$

Diffraction from a modulation

For simple a 1D modulated structure, we can compute the scattering assuming

$$x_n = an + u \cos(qan)$$

and that the scattering factor for each atom is set to unity

for the displacement u small, this becomes

$$A(Q) = \sum_{n=0}^{N-1} e^{iQx_n} = \sum_{n=0}^{N-1} e^{iQ(an + \cos(qan))}$$

$$= \sum_{n=0}^{N-1} e^{iQan} e^{iQu \cos(qan)}$$

$$A(Q) \approx \sum_{n=0}^{N-1} e^{iQan} [1 + iQu \cos(qan) + \dots]$$

$$A(Q) \approx \sum_{n=0}^{N-1} e^{iQan} + i \left(\frac{Qu}{2} \right) \left[e^{i(Q+q)an} + e^{-i(Q-q)an} \right]$$

$$I(Q) = N \left(\frac{2\pi}{a} \right) \sum_h \delta(Q - G_h) + \left(\frac{Qu}{2} \right)^2 \left[\delta(Q + q - G_h) + \delta(Q - q - G_h) \right]$$

Diffraction from a modulation

For simple a 1D modulated structure, we can compute the scattering assuming

$$x_n = an + u \cos(qan)$$

and that the scattering factor for each atom is set to unity

for the displacement u small, this becomes

$$A(Q) = \sum_{n=0}^{N-1} e^{iQx_n} = \sum_{n=0}^{N-1} e^{iQ(an + \cos(qan))}$$

$$= \sum_{n=0}^{N-1} e^{iQan} e^{iQu \cos(qan)}$$

$$A(Q) \approx \sum_{n=0}^{N-1} e^{iQan} [1 + iQu \cos(qan) + \dots]$$

$$A(Q) \approx \sum_{n=0}^{N-1} e^{iQan} + i \left(\frac{Qu}{2} \right) \left[e^{i(Q+q)an} + e^{-i(Q-q)an} \right]$$

$$I(Q) = N \left(\frac{2\pi}{a} \right) \sum_h \delta(Q - G_h) + \left(\frac{Qu}{2} \right)^2 \left[\delta(Q + q - G_h) + \delta(Q - q - G_h) \right]$$

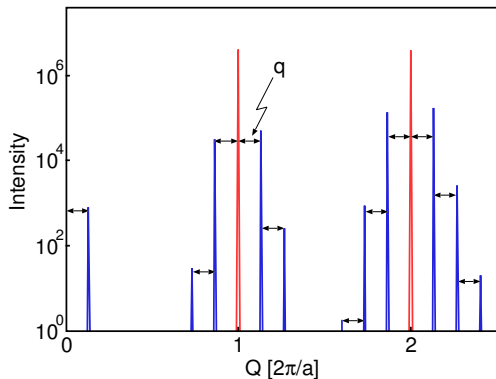
the diffraction pattern has **main** Bragg peaks plus **satellite** peaks

Quasiperiodic scattering

$$I(Q) = N \left(\frac{2\pi}{a} \right) \sum_h \delta(Q - G_h) + \left(\frac{Qu}{2} \right)^2 \left[\delta(Q + q - G_h) + \delta(Q - q - G_h) \right]$$

Quasiperiodic scattering

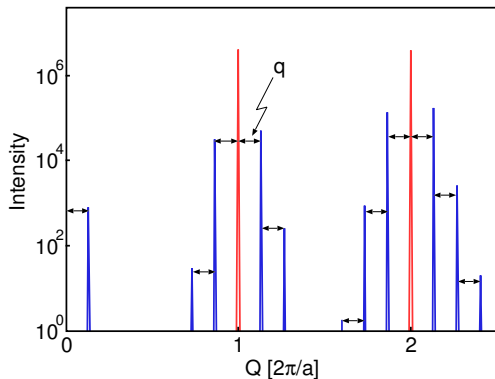
$$I(Q) = N \left(\frac{2\pi}{a} \right) \sum_h \delta(Q - G_h) + \left(\frac{Qu}{2} \right)^2 \left[\delta(Q + q - G_h) + \delta(Q - q - G_h) \right]$$



Quasiperiodic scattering

$$I(Q) = N \left(\frac{2\pi}{a} \right) \sum_h \delta(Q - G_h) + \left(\frac{Qu}{2} \right)^2 \left[\delta(Q + q - G_h) + \delta(Q - q - G_h) \right]$$

This kind of scattering pattern holds for both commensurate and incommensurate modulations and there are multiple satellites around the $Q = 0$ as well as every main peak

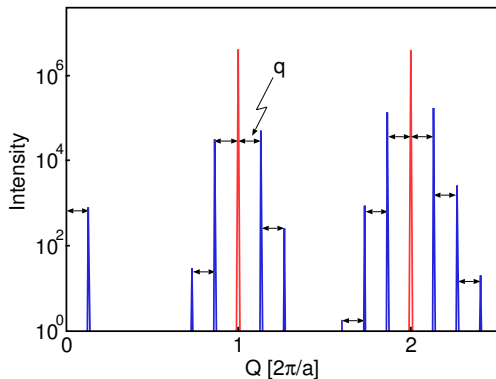


Quasiperiodic scattering

$$I(Q) = N \left(\frac{2\pi}{a} \right) \sum_h \delta(Q - G_h) + \left(\frac{Qu}{2} \right)^2 \left[\delta(Q + q - G_h) + \delta(Q - q - G_h) \right]$$

This kind of scattering pattern holds for both commensurate and incommensurate modulations and there are multiple satellites around the $Q = 0$ as well as every main peak

If the modulation of the structure is a multiple of the lattice parameter, the modulation is simply a superlattice and the actual lattice parameter will be changed.



Quasicrystals

The only rotational symmetries which permit a space-filling lattice are 2-, 3-, 4-, and 6-fold.

Quasicrystals

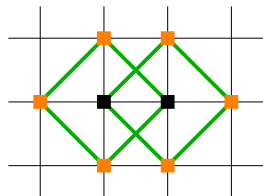
The only rotational symmetries which permit a space-filling lattice are 2-, 3-, 4-, and 6-fold.

In 1984, D. Schechtman and co-workers reported the first observation of a “crystal” with long range order but no translational symmetry in rapidly cooled $\text{Al}_{86}\text{Mn}_{14}$.

Quasicrystals

The only rotational symmetries which permit a space-filling lattice are 2-, 3-, 4-, and 6-fold.

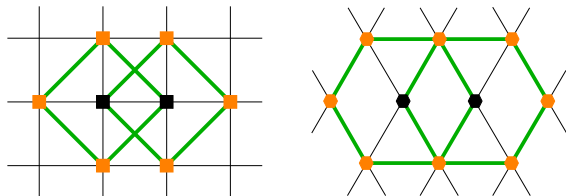
In 1984, D. Schechtman and co-workers reported the first observation of a “crystal” with long range order but no translational symmetry in rapidly cooled $\text{Al}_{86}\text{Mn}_{14}$.



Quasicrystals

The only rotational symmetries which permit a space-filling lattice are 2-, 3-, 4-, and 6-fold.

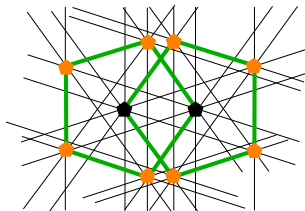
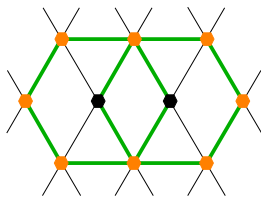
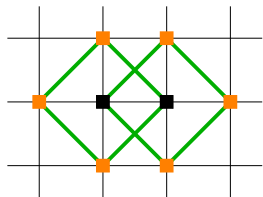
In 1984, D. Schechtman and co-workers reported the first observation of a “crystal” with long range order but no translational symmetry in rapidly cooled $\text{Al}_{86}\text{Mn}_{14}$.



Quasicrystals

The only rotational symmetries which permit a space-filling lattice are 2-, 3-, 4-, and 6-fold.

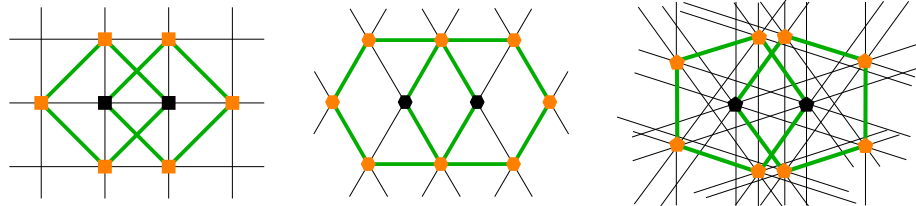
In 1984, D. Schechtman and co-workers reported the first observation of a “crystal” with long range order but no translational symmetry in rapidly cooled $\text{Al}_{86}\text{Mn}_{14}$.



Quasicrystals

The only rotational symmetries which permit a space-filling lattice are 2-, 3-, 4-, and 6-fold.

In 1984, D. Schechtman and co-workers reported the first observation of a “crystal” with long range order but no translational symmetry in rapidly cooled $\text{Al}_{86}\text{Mn}_{14}$.

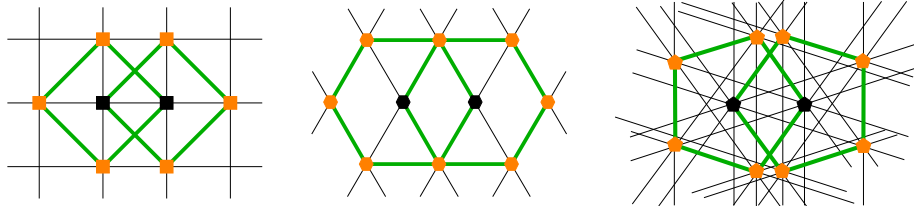


Initially this result was not accepted but as many new materials with the same were discovered it was clear that a new kind of crystal had been discovered.

Quasicrystals

The only rotational symmetries which permit a space-filling lattice are 2-, 3-, 4-, and 6-fold.

In 1984, D. Schechtman and co-workers reported the first observation of a “crystal” with long range order but no translational symmetry in rapidly cooled $\text{Al}_{86}\text{Mn}_{14}$.

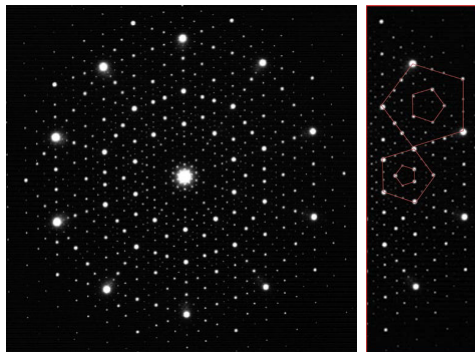


Initially this result was not accepted but as many new materials with the same were discovered it was clear that a new kind of crystal had been discovered.

In 2011 Shechtman was awarded the Nobel Prize in Chemistry

5-fold symmetry

The electron micrographs show that there must be long range order to be able to get such sharp diffraction peaks

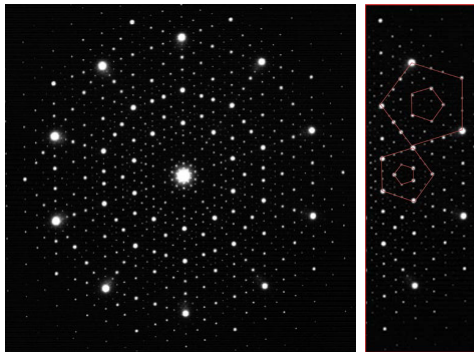


"Metallic phase with long-range orientational order and no translational symmetry," D. Shechtman, I. Blech, D. Gratias, and J.W. Cahn, *Phys. Rev. Lett.* **53**, 1951-1953 (1984)

5-fold symmetry

The electron micrographs show that there must be long range order to be able to get such sharp diffraction peaks

The 5-fold symmetry is evident in the 10 spots surrounding the center of the left image and the pentagonal arrangements of atoms in the image on the right.

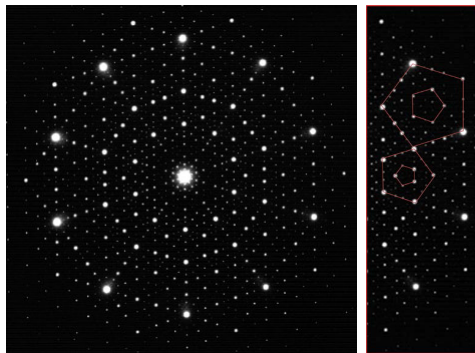


"Metallic phase with long-range orientational order and no translational symmetry," D. Shechtman, I. Blech, D. Gratias, and J.W. Cahn, *Phys. Rev. Lett.* **53**, 1951-1953 (1984)

5-fold symmetry

The electron micrographs show that there must be long range order to be able to get such sharp diffraction peaks

The 5-fold symmetry is evident in the 10 spots surrounding the center of the left image and the pentagonal arrangements of atoms in the image on the right.



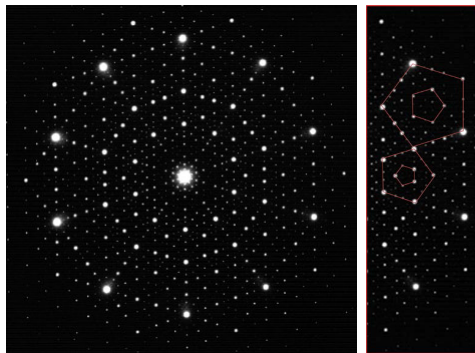
This metastable phase was also found with Fe and Cr in the place of Mn.

"Metallic phase with long-range orientational order and no translational symmetry," D. Shechtman, I. Blech, D. Gratias, and J.W. Cahn, *Phys. Rev. Lett.* **53**, 1951-1953 (1984)

5-fold symmetry

The electron micrographs show that there must be long range order to be able to get such sharp diffraction peaks

The 5-fold symmetry is evident in the 10 spots surrounding the center of the left image and the pentagonal arrangements of atoms in the image on the right.



This metastable phase was also found with Fe and Cr in the place of Mn.

Other groups have discovered stable icosahedral phases with three and two elements.

"Metallic phase with long-range orientational order and no translational symmetry," D. Shechtman, I. Blech, D. Gratias, and J.W. Cahn, *Phys. Rev. Lett.* **53**, 1951-1953 (1984)

Quasicrystal diffraction patterns

The $\text{Al}_{65}\text{Cu}_{20}\text{Fe}_{15}$ system was one of the first stable quasicrystals to be discovered. Later discovery of stable quasicrystals in the Ta-Te, Cd-Ca, and Cd-Yb systems enabled large crystals to be grown.

"A stable quasicrystal in Al-Cu-Fe system," A.-P. Tsai, A. Inoue, and T. Masumoto, *Jap. J. Appl. Phys.* **26**, L1505 (1987)

Quasicrystal diffraction patterns

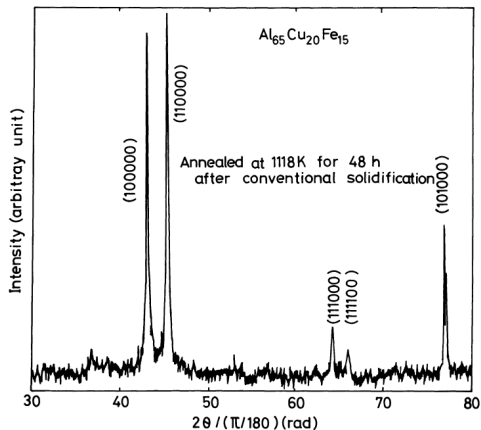
The $\text{Al}_{65}\text{Cu}_{20}\text{Fe}_{15}$ system was one of the first stable quasicrystals to be discovered. Later discovery of stable quasicrystals in the Ta-Te, Cd-Ca, and Cd-Yb systems enabled large crystals to be grown.

The diffraction pattern and SEM images show the hallmark of an icosahedral crystal

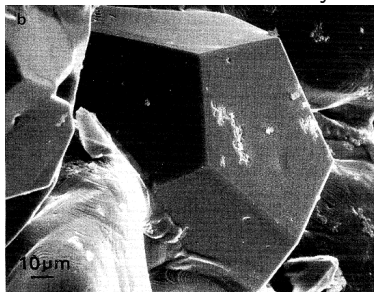
"A stable quasicrystal in Al-Cu-Fe system," A.-P. Tsai, A. Inoue, and T. Masumoto, *Jap. J. Appl. Phys.* **26**, L1505 (1987)

Quasicrystal diffraction patterns

The $\text{Al}_{65}\text{Cu}_{20}\text{Fe}_{15}$ system was one of the first stable quasicrystals to be discovered. Later discovery of stable quasicrystals in the Ta-Te, Cd-Ca, and Cd-Yb systems enabled large crystals to be grown.



The diffraction pattern and SEM images show the hallmark of an icosahedral crystal



"A stable quasicrystal in Al-Cu-Fe system," A.-P. Tsai, A. Inoue, and T. Masumoto, *Jap. J. Appl. Phys.* **26**, L1505 (1987)

Lattice Vibrations

Atoms on a lattice are not rigid but vibrate. There is zero-point motion as well as thermal motion. These vibrations influence the x-ray scattering.

Lattice Vibrations

Atoms on a lattice are not rigid but vibrate. There is zero-point motion as well as thermal motion. These vibrations influence the x-ray scattering.

For a 1D lattice, we replace the position of the atom with its *instantaneous* position, $\vec{R}_n + \vec{u}_n$ where \vec{u}_n is the displacement from the equilibrium position, \vec{R}_n .

Lattice Vibrations

Atoms on a lattice are not rigid but vibrate. There is zero-point motion as well as thermal motion. These vibrations influence the x-ray scattering.

For a 1D lattice, we replace the position of the atom with its *instantaneous* position, $\vec{R}_n + \vec{u}_n$ where \vec{u}_n is the displacement from the equilibrium position, \vec{R}_n . Computing the intensity:

Lattice Vibrations

Atoms on a lattice are not rigid but vibrate. There is zero-point motion as well as thermal motion. These vibrations influence the x-ray scattering.

For a 1D lattice, we replace the position of the atom with its *instantaneous* position, $\vec{R}_n + \vec{u}_n$ where \vec{u}_n is the displacement from the equilibrium position, \vec{R}_n . Computing the intensity:

$$I = \left\langle \sum_m f(\vec{Q}) e^{i\vec{Q}\cdot(\vec{R}_m + \vec{u}_m)} \sum_n f^*(\vec{Q}) e^{-i\vec{Q}\cdot(\vec{R}_n + \vec{u}_n)} \right\rangle$$

Lattice Vibrations

Atoms on a lattice are not rigid but vibrate. There is zero-point motion as well as thermal motion. These vibrations influence the x-ray scattering.

For a 1D lattice, we replace the position of the atom with its *instantaneous* position, $\vec{R}_n + \vec{u}_n$ where \vec{u}_n is the displacement from the equilibrium position, \vec{R}_n . Computing the intensity:

$$\begin{aligned} I &= \left\langle \sum_m f(\vec{Q}) e^{i\vec{Q}\cdot(\vec{R}_m + \vec{u}_m)} \sum_n f^*(\vec{Q}) e^{-i\vec{Q}\cdot(\vec{R}_n + \vec{u}_n)} \right\rangle \\ &= \sum_m \sum_n f(\vec{Q}) f^*(\vec{Q}) e^{i\vec{Q}\cdot(\vec{R}_m - \vec{R}_n)} \left\langle e^{i\vec{Q}\cdot(\vec{u}_m - \vec{u}_n)} \right\rangle \end{aligned}$$

Lattice Vibrations

Atoms on a lattice are not rigid but vibrate. There is zero-point motion as well as thermal motion. These vibrations influence the x-ray scattering.

For a 1D lattice, we replace the position of the atom with its *instantaneous* position, $\vec{R}_n + \vec{u}_n$ where \vec{u}_n is the displacement from the equilibrium position, \vec{R}_n . Computing the intensity:

$$\begin{aligned} I &= \left\langle \sum_m f(\vec{Q}) e^{i\vec{Q}\cdot(\vec{R}_m + \vec{u}_m)} \sum_n f^*(\vec{Q}) e^{-i\vec{Q}\cdot(\vec{R}_n + \vec{u}_n)} \right\rangle \\ &= \sum_m \sum_n f(\vec{Q}) f^*(\vec{Q}) e^{i\vec{Q}\cdot(\vec{R}_m - \vec{R}_n)} \left\langle e^{i\vec{Q}\cdot(\vec{u}_m - \vec{u}_n)} \right\rangle \end{aligned}$$

The last term is a time average which can be simplified using the Baker-Hausdorff theorem, $\langle e^{ix} \rangle = e^{-\langle x^2 \rangle / 2}$

Lattice Vibrations

Atoms on a lattice are not rigid but vibrate. There is zero-point motion as well as thermal motion. These vibrations influence the x-ray scattering.

For a 1D lattice, we replace the position of the atom with its *instantaneous* position, $\vec{R}_n + \vec{u}_n$ where \vec{u}_n is the displacement from the equilibrium position, \vec{R}_n . Computing the intensity:

$$\begin{aligned} I &= \left\langle \sum_m f(\vec{Q}) e^{i\vec{Q}\cdot(\vec{R}_m + \vec{u}_m)} \sum_n f^*(\vec{Q}) e^{-i\vec{Q}\cdot(\vec{R}_n + \vec{u}_n)} \right\rangle \\ &= \sum_m \sum_n f(\vec{Q}) f^*(\vec{Q}) e^{i\vec{Q}\cdot(\vec{R}_m - \vec{R}_n)} \left\langle e^{i\vec{Q}\cdot(\vec{u}_m - \vec{u}_n)} \right\rangle \end{aligned}$$

The last term is a time average which can be simplified using the Baker-Hausdorff theorem, $\langle e^{ix} \rangle = e^{-\langle x^2 \rangle / 2}$

$$\left\langle e^{i\vec{Q}\cdot(\vec{u}_m - \vec{u}_n)} \right\rangle = \left\langle e^{iQ(u_{Qm} - u_{Qn})} \right\rangle$$

Lattice Vibrations

Atoms on a lattice are not rigid but vibrate. There is zero-point motion as well as thermal motion. These vibrations influence the x-ray scattering.

For a 1D lattice, we replace the position of the atom with its *instantaneous* position, $\vec{R}_n + \vec{u}_n$ where \vec{u}_n is the displacement from the equilibrium position, \vec{R}_n . Computing the intensity:

$$\begin{aligned} I &= \left\langle \sum_m f(\vec{Q}) e^{i\vec{Q}\cdot(\vec{R}_m + \vec{u}_m)} \sum_n f^*(\vec{Q}) e^{-i\vec{Q}\cdot(\vec{R}_n + \vec{u}_n)} \right\rangle \\ &= \sum_m \sum_n f(\vec{Q}) f^*(\vec{Q}) e^{i\vec{Q}\cdot(\vec{R}_m - \vec{R}_n)} \left\langle e^{i\vec{Q}\cdot(\vec{u}_m - \vec{u}_n)} \right\rangle \end{aligned}$$

The last term is a time average which can be simplified using the Baker-Hausdorff theorem, $\langle e^{ix} \rangle = e^{-\langle x^2 \rangle / 2}$

$$\left\langle e^{i\vec{Q}\cdot(\vec{u}_m - \vec{u}_n)} \right\rangle = \left\langle e^{iQ(u_{Qm} - u_{Qn})} \right\rangle = e^{-\langle Q^2 (u_{Qm} - u_{Qn})^2 \rangle / 2}$$

Lattice Vibrations

$$\langle e^{iQ(u_{Qm}-u_{Qn})} \rangle = e^{-Q^2 \langle u_{Qm}^2 \rangle / 2} e^{-Q^2 \langle u_{Qn}^2 \rangle / 2} e^{Q^2 \langle u_{Qm} u_{Qn} \rangle}$$

Lattice Vibrations

$$\begin{aligned}\langle e^{iQ(u_{Qm}-u_{Qn})} \rangle &= e^{-Q^2\langle u_{Qm}^2 \rangle/2} e^{-Q^2\langle u_{Qn}^2 \rangle/2} e^{Q^2\langle u_{Qm}u_{Qn} \rangle} \\ &= e^{-Q^2\langle u_Q^2 \rangle} e^{Q^2\langle u_{Qm}u_{Qn} \rangle}\end{aligned}$$

Lattice Vibrations

$$\begin{aligned}\langle e^{iQ(u_{Qm}-u_{Qn})} \rangle &= e^{-Q^2\langle u_{Qm}^2 \rangle/2} e^{-Q^2\langle u_{Qn}^2 \rangle/2} e^{Q^2\langle u_{Qm}u_{Qn} \rangle} \\ &= e^{-Q^2\langle u_Q^2 \rangle} e^{Q^2\langle u_{Qm}u_{Qn} \rangle} = e^{-2M} e^{Q^2\langle u_{Qm}u_{Qn} \rangle}\end{aligned}$$

Lattice Vibrations

$$\begin{aligned}\langle e^{iQ(u_{Qm}-u_{Qn})} \rangle &= e^{-Q^2\langle u_{Qm}^2 \rangle/2} e^{-Q^2\langle u_{Qn}^2 \rangle/2} e^{Q^2\langle u_{Qm}u_{Qn} \rangle} \\ &= e^{-Q^2\langle u_Q^2 \rangle} e^{Q^2\langle u_{Qm}u_{Qn} \rangle} = e^{-2M} e^{Q^2\langle u_{Qm}u_{Qn} \rangle} \\ &= e^{-2M} \left[1 + e^{Q^2\langle u_{Qm}u_{Qn} \rangle} - 1 \right]\end{aligned}$$

Lattice Vibrations

$$\begin{aligned}\langle e^{iQ(u_{Qm}-u_{Qn})} \rangle &= e^{-Q^2\langle u_{Qm}^2 \rangle/2} e^{-Q^2\langle u_{Qn}^2 \rangle/2} e^{Q^2\langle u_{Qm}u_{Qn} \rangle} \\ &= e^{-Q^2\langle u_Q^2 \rangle} e^{Q^2\langle u_{Qm}u_{Qn} \rangle} = e^{-2M} e^{Q^2\langle u_{Qm}u_{Qn} \rangle} \\ &= e^{-2M} \left[1 + e^{Q^2\langle u_{Qm}u_{Qn} \rangle} - 1 \right]\end{aligned}$$

Substituting into the expression for intensity

Lattice Vibrations

$$\begin{aligned}\left\langle e^{iQ(u_{Qm}-u_{Qn})} \right\rangle &= e^{-Q^2\langle u_{Qm}^2 \rangle/2} e^{-Q^2\langle u_{Qn}^2 \rangle/2} e^{Q^2\langle u_{Qm}u_{Qn} \rangle} \\ &= e^{-Q^2\langle u_Q^2 \rangle} e^{Q^2\langle u_{Qm}u_{Qn} \rangle} = e^{-2M} e^{Q^2\langle u_{Qm}u_{Qn} \rangle} \\ &= e^{-2M} \left[1 + e^{Q^2\langle u_{Qm}u_{Qn} \rangle} - 1 \right]\end{aligned}$$

Substituting into the expression for intensity

$$\begin{aligned}I &= \sum_m \sum_n f(\vec{Q}) e^{-M} e^{i\vec{Q}\cdot\vec{R}_m} f^*(\vec{Q}) e^{-M} e^{-i\vec{Q}\cdot\vec{R}_n} \\ &+ \sum_m \sum_n f(\vec{Q}) e^{-M} e^{i\vec{Q}\cdot\vec{R}_m} f^*(\vec{Q}) e^{-M} e^{-i\vec{Q}\cdot\vec{R}_n} \left[e^{Q^2\langle u_{Qm}u_{Qn} \rangle} - 1 \right]\end{aligned}$$

Lattice Vibrations

$$\begin{aligned}\langle e^{iQ(u_{Qm}-u_{Qn})} \rangle &= e^{-Q^2\langle u_{Qm}^2 \rangle/2} e^{-Q^2\langle u_{Qn}^2 \rangle/2} e^{Q^2\langle u_{Qm}u_{Qn} \rangle} \\ &= e^{-Q^2\langle u_Q^2 \rangle} e^{Q^2\langle u_{Qm}u_{Qn} \rangle} = e^{-2M} e^{Q^2\langle u_{Qm}u_{Qn} \rangle} \\ &= e^{-2M} \left[1 + e^{Q^2\langle u_{Qm}u_{Qn} \rangle} - 1 \right]\end{aligned}$$

Substituting into the expression for intensity

$$\begin{aligned}I &= \sum_m \sum_n f(\vec{Q}) e^{-M} e^{i\vec{Q}\cdot\vec{R}_m} f^*(\vec{Q}) e^{-M} e^{-i\vec{Q}\cdot\vec{R}_n} \\ &+ \sum_m \sum_n f(\vec{Q}) e^{-M} e^{i\vec{Q}\cdot\vec{R}_m} f^*(\vec{Q}) e^{-M} e^{-i\vec{Q}\cdot\vec{R}_n} \left[e^{Q^2\langle u_{Qm}u_{Qn} \rangle} - 1 \right]\end{aligned}$$

The first term is just the elastic scattering from the lattice with the addition of the term $e^{-M} = e^{-Q^2\langle u_Q^2 \rangle/2}$, called the Debye-Waller factor.

Lattice Vibrations

$$\begin{aligned}\langle e^{i\mathbf{Q}(u_{Qm}-u_{Qn})} \rangle &= e^{-Q^2\langle u_{Qm}^2 \rangle/2} e^{-Q^2\langle u_{Qn}^2 \rangle/2} e^{Q^2\langle u_{Qm}u_{Qn} \rangle} \\ &= e^{-Q^2\langle u_Q^2 \rangle} e^{Q^2\langle u_{Qm}u_{Qn} \rangle} = e^{-2M} e^{Q^2\langle u_{Qm}u_{Qn} \rangle} \\ &= e^{-2M} \left[1 + e^{Q^2\langle u_{Qm}u_{Qn} \rangle} - 1 \right]\end{aligned}$$

Substituting into the expression for intensity

$$\begin{aligned}I &= \sum_m \sum_n f(\vec{Q}) e^{-M} e^{i\vec{Q}\cdot\vec{R}_m} f^*(\vec{Q}) e^{-M} e^{-i\vec{Q}\cdot\vec{R}_n} \\ &+ \sum_m \sum_n f(\vec{Q}) e^{-M} e^{i\vec{Q}\cdot\vec{R}_m} f^*(\vec{Q}) e^{-M} e^{-i\vec{Q}\cdot\vec{R}_n} \left[e^{Q^2\langle u_{Qm}u_{Qn} \rangle} - 1 \right]\end{aligned}$$

The first term is just the elastic scattering from the lattice with the addition of the term $e^{-M} = e^{-Q^2\langle u_Q^2 \rangle/2}$, called the Debye-Waller factor.

The second term is the Thermal Diffuse Scattering and actually increases with mean squared displacement.

Thermal Diffuse Scattering

$$I^{TDS} = \sum_m \sum_n f(\vec{Q}) e^{-M} e^{i\vec{Q}\cdot\vec{R}_m} f^*(\vec{Q}) e^{-M} e^{-i\vec{Q}\cdot\vec{R}_n} \left[e^{Q^2 \langle u_{Qm} u_{Qn} \rangle} - 1 \right]$$

Thermal Diffuse Scattering

$$I^{TDS} = \sum_m \sum_n f(\vec{Q}) e^{-M} e^{i\vec{Q}\cdot\vec{R}_m} f^*(\vec{Q}) e^{-M} e^{-i\vec{Q}\cdot\vec{R}_n} \left[e^{Q^2 \langle u_{Qm} u_{Qn} \rangle} - 1 \right]$$

The TDS has a width determined by the **correlated displacement of atoms** which is much broader than a Bragg peak.

Thermal Diffuse Scattering

$$I^{TDS} = \sum_m \sum_n f(\vec{Q}) e^{-M} e^{i\vec{Q}\cdot\vec{R}_m} f^*(\vec{Q}) e^{-M} e^{-i\vec{Q}\cdot\vec{R}_n} \left[e^{Q^2 \langle u_{Qm} u_{Qn} \rangle} - 1 \right]$$

The TDS has a width determined by the **correlated displacement of atoms** which is much broader than a Bragg peak.

These correlated motions are just phonons.

Thermal Diffuse Scattering

$$I^{TDS} = \sum_m \sum_n f(\vec{Q}) e^{-M} e^{i\vec{Q}\cdot\vec{R}_m} f^*(\vec{Q}) e^{-M} e^{-i\vec{Q}\cdot\vec{R}_n} \left[e^{Q^2 \langle u_{Qm} u_{Qn} \rangle} - 1 \right]$$

The TDS has a width determined by the **correlated displacement of atoms** which is much broader than a Bragg peak.

These correlated motions are just phonons.

A 0.5mm Si wafer illuminated by 28keV x-rays from an APS undulator were used to measure the phonon dispersion curves of silicon

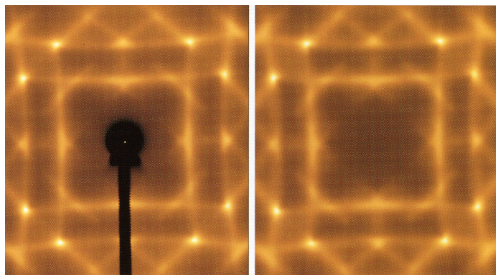
Thermal Diffuse Scattering

$$I^{TDS} = \sum_m \sum_n f(\vec{Q}) e^{-M} e^{i\vec{Q}\cdot\vec{R}_m} f^*(\vec{Q}) e^{-M} e^{-i\vec{Q}\cdot\vec{R}_n} \left[e^{Q^2 \langle u_{Qm} u_{Qn} \rangle} - 1 \right]$$

The TDS has a width determined by the **correlated displacement of atoms** which is much broader than a Bragg peak.

These correlated motions are just phonons.

A 0.5mm Si wafer illuminated by 28keV x-rays from an APS undulator were used to measure the phonon dispersion curves of silicon



incident beam along (100)

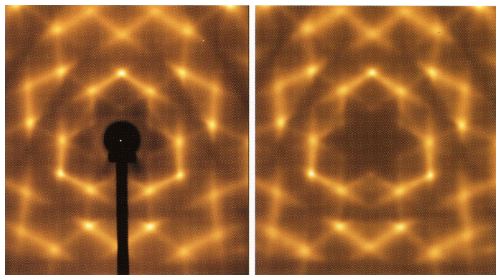
Thermal Diffuse Scattering

$$I^{TDS} = \sum_m \sum_n f(\vec{Q}) e^{-M} e^{i\vec{Q}\cdot\vec{R}_m} f^*(\vec{Q}) e^{-M} e^{-i\vec{Q}\cdot\vec{R}_n} \left[e^{Q^2 \langle u_{Qm} u_{Qn} \rangle} - 1 \right]$$

The TDS has a width determined by the **correlated displacement of atoms** which is much broader than a Bragg peak.

These correlated motions are just phonons.

A 0.5mm Si wafer illuminated by 28keV x-rays from an APS undulator were used to measure the phonon dispersion curves of silicon



incident beam along (111)

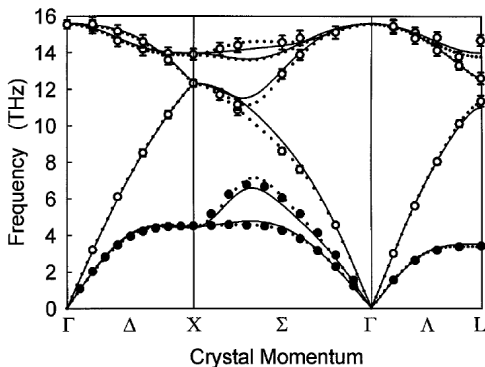
Thermal Diffuse Scattering

$$I^{TDS} = \sum_m \sum_n f(\vec{Q}) e^{-M} e^{i\vec{Q}\cdot\vec{R}_m} f^*(\vec{Q}) e^{-M} e^{-i\vec{Q}\cdot\vec{R}_n} \left[e^{Q^2 \langle u_{Qm} u_{Qn} \rangle} - 1 \right]$$

The TDS has a width determined by the **correlated displacement of atoms** which is much broader than a Bragg peak.

These correlated motions are just phonons.

A 0.5mm Si wafer illuminated by 28keV x-rays from an APS undulator were used to measure the phonon dispersion curves of silicon



dotted line from this measurement

Properties of the Debye-Waller Factor

For crystals with several different types of atoms, we generalize the unit cell scattering factor.

Properties of the Debye-Waller Factor

For crystals with several different types of atoms, we generalize the unit cell scattering factor.

$$F^{u.c.} = \sum_j f_j(\vec{Q}) e^{-M_j} e^{i\vec{Q}\cdot\vec{r}_j}$$

Properties of the Debye-Waller Factor

For crystals with several different types of atoms, we generalize the unit cell scattering factor.

$$F^{u.c.} = \sum_j f_j(\vec{Q}) e^{-M_j} e^{i\vec{Q}\cdot\vec{r}_j}$$
$$M_j = \frac{1}{2} Q^2 \langle u_{Qj}^2 \rangle$$

Properties of the Debye-Waller Factor

For crystals with several different types of atoms, we generalize the unit cell scattering factor.

$$F^{u.c.} = \sum_j f_j(\vec{Q}) e^{-M_j} e^{i\vec{Q}\cdot\vec{r}_j}$$
$$M_j = \frac{1}{2} Q^2 \langle u_{Qj}^2 \rangle$$
$$= \frac{1}{2} \left(\frac{4\pi}{\lambda} \right)^2 \sin^2 \theta \langle u_{Qj}^2 \rangle$$

Properties of the Debye-Waller Factor

For crystals with several different types of atoms, we generalize the unit cell scattering factor.

$$B_T^j = 8\pi^2 \langle u_{Qj}^2 \rangle$$

$$\begin{aligned} F^{u.c.} &= \sum_j f_j(\vec{Q}) e^{-M_j} e^{i\vec{Q}\cdot\vec{r}_j} \\ M_j &= \frac{1}{2} Q^2 \langle u_{Qj}^2 \rangle \\ &= \frac{1}{2} \left(\frac{4\pi}{\lambda} \right)^2 \sin^2 \theta \langle u_{Qj}^2 \rangle \\ M_j &= B_T^j \left(\frac{\sin \theta}{\lambda} \right)^2 \end{aligned}$$

Properties of the Debye-Waller Factor

For crystals with several different types of atoms, we generalize the unit cell scattering factor.

$$B_T^j = 8\pi^2 \langle u_{Qj}^2 \rangle$$

for isotropic atomic vibrations

$$\begin{aligned} \langle u^2 \rangle &= \langle u_x^2 + u_y^2 + u_z^2 \rangle \\ &= 3\langle u_x^2 \rangle = 3\langle u_Q^2 \rangle \end{aligned}$$

$$F^{u.c.} = \sum_j f_j(\vec{Q}) e^{-M_j} e^{i\vec{Q} \cdot \vec{r}_j}$$

$$\begin{aligned} M_j &= \frac{1}{2} Q^2 \langle u_{Qj}^2 \rangle \\ &= \frac{1}{2} \left(\frac{4\pi}{\lambda} \right)^2 \sin^2 \theta \langle u_{Qj}^2 \rangle \end{aligned}$$

$$M_j = B_T^j \left(\frac{\sin \theta}{\lambda} \right)^2$$

Properties of the Debye-Waller Factor

For crystals with several different types of atoms, we generalize the unit cell scattering factor.

$$B_T^j = 8\pi^2 \langle u_{Qj}^2 \rangle$$

for isotropic atomic vibrations

$$\begin{aligned} \langle u^2 \rangle &= \langle u_x^2 + u_y^2 + u_z^2 \rangle \\ &= 3\langle u_x^2 \rangle = 3\langle u_Q^2 \rangle \end{aligned}$$

$$F^{u.c.} = \sum_j f_j(\vec{Q}) e^{-M_j} e^{i\vec{Q} \cdot \vec{r}_j}$$

$$\begin{aligned} M_j &= \frac{1}{2} Q^2 \langle u_{Qj}^2 \rangle \\ &= \frac{1}{2} \left(\frac{4\pi}{\lambda} \right)^2 \sin^2 \theta \langle u_{Qj}^2 \rangle \end{aligned}$$

$$M_j = B_T^j \left(\frac{\sin \theta}{\lambda} \right)^2$$

$$B_T^{iso} = \frac{8\pi^2}{3} \langle u^2 \rangle$$

Properties of the Debye-Waller Factor

For crystals with several different types of atoms, we generalize the unit cell scattering factor.

$$B_T^j = 8\pi^2 \langle u_{Qj}^2 \rangle$$

for isotropic atomic vibrations

$$\begin{aligned} \langle u^2 \rangle &= \langle u_x^2 + u_y^2 + u_z^2 \rangle \\ &= 3\langle u_x^2 \rangle = 3\langle u_Q^2 \rangle \end{aligned}$$

$$F^{u.c.} = \sum_j f_j(\vec{Q}) e^{-M_j} e^{i\vec{Q} \cdot \vec{r}_j}$$

$$\begin{aligned} M_j &= \frac{1}{2} Q^2 \langle u_{Qj}^2 \rangle \\ &= \frac{1}{2} \left(\frac{4\pi}{\lambda} \right)^2 \sin^2 \theta \langle u_{Qj}^2 \rangle \end{aligned}$$

$$M_j = B_T^j \left(\frac{\sin \theta}{\lambda} \right)^2$$

$$B_T^{iso} = \frac{8\pi^2}{3} \langle u^2 \rangle$$

In general, Debye-Waller factors can be anisotropic

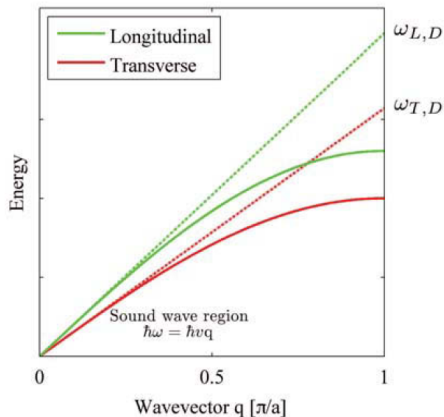
The Debye Model

The Debye model can be used to compute B_T by integrating a linear phonon dispersion relation up to a cutoff frequency, ω_D , called the Debye frequency.

The Debye Model

The Debye model can be used to compute B_T by integrating a linear phonon dispersion relation up to a cutoff frequency, ω_D , called the Debye frequency.

B_T is given as a function of the Debye temperature Θ .

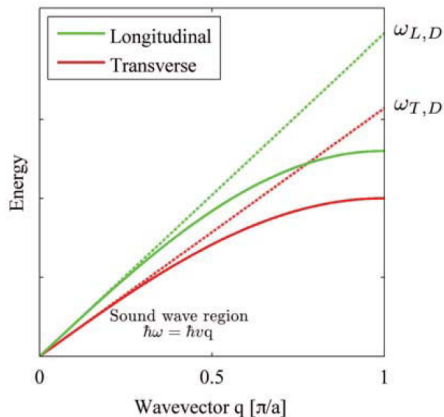


The Debye Model

The Debye model can be used to compute B_T by integrating a linear phonon dispersion relation up to a cutoff frequency, ω_D , called the Debye frequency.

B_T is given as a function of the Debye temperature Θ .

$$B_T = \frac{6h^2}{m_A k_B \Theta} \left[\frac{\phi(\Theta/T)}{\Theta/T} + \frac{1}{4} \right]$$



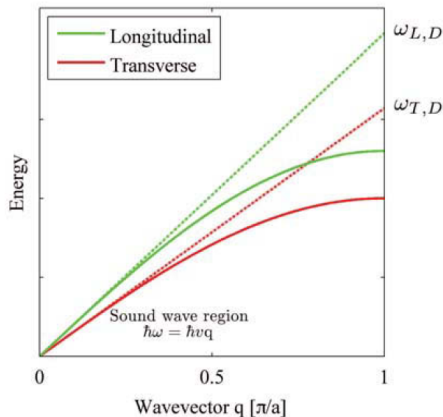
The Debye Model

The Debye model can be used to compute B_T by integrating a linear phonon dispersion relation up to a cutoff frequency, ω_D , called the Debye frequency.

B_T is given as a function of the Debye temperature Θ .

$$B_T = \frac{6h^2}{m_A k_B \Theta} \left[\frac{\phi(\Theta/T)}{\Theta/T} + \frac{1}{4} \right]$$

$$\phi(x) = \frac{1}{x} \int_0^{\Theta/T} \frac{\xi}{e^\xi - 1} d\xi$$



The Debye Model

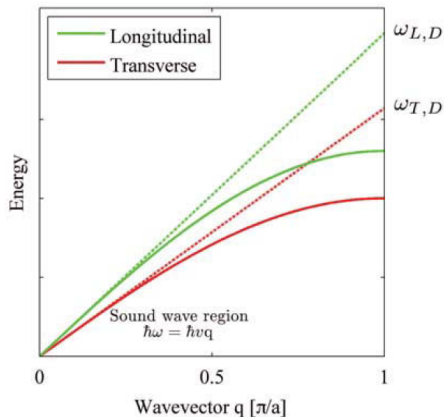
The Debye model can be used to compute B_T by integrating a linear phonon dispersion relation up to a cutoff frequency, ω_D , called the Debye frequency.

B_T is given as a function of the Debye temperature Θ .

$$B_T = \frac{6h^2}{m_A k_B \Theta} \left[\frac{\phi(\Theta/T)}{\Theta/T} + \frac{1}{4} \right]$$

$$\phi(x) = \frac{1}{x} \int_0^{\Theta/T} \frac{\xi}{e^\xi - 1} d\xi$$

$$B_T [\text{\AA}^2] = \frac{11492 T [\text{K}]}{A \Theta^2 [\text{K}^2]} \phi(\Theta/T) + \frac{2873}{A \Theta [\text{K}]}$$



Debye Temperatures

$$B_T = \frac{11492T}{A\Theta^2} \phi(\Theta/T) + \frac{2873}{A\Theta}$$

	A	Θ (K)	$B_{4.2}$	B_{77} (\AA^2)	B_{293}
C*	12	2230	0.11	0.11	0.12
Al	27	428	0.25	0.30	0.72
Cu	63.5	343	0.13	0.17	0.47

*diamond

Debye Temperatures

$$B_T = \frac{11492T}{A\Theta^2} \phi(\Theta/T) + \frac{2873}{A\Theta}$$

	A	Θ (K)	$B_{4.2}$	B_{77} (\AA^2)	B_{293}
C*	12	2230	0.11	0.11	0.12
Al	27	428	0.25	0.30	0.72
Cu	63.5	343	0.13	0.17	0.47

*diamond

diamond is very stiff and Θ does not vary much with temperature

Debye Temperatures

$$B_T = \frac{11492T}{A\Theta^2} \phi(\Theta/T) + \frac{2873}{A\Theta}$$

	A	Θ (K)	$B_{4.2}$	B_{77} (\AA^2)	B_{293}
C*	12	2230	0.11	0.11	0.12
Al	27	428	0.25	0.30	0.72
Cu	63.5	343	0.13	0.17	0.47

*diamond

diamond is very stiff and Θ does not vary much with temperature

copper has a much lower Debye temperature and a wider variation of thermal factor with temperature

Debye Temperatures

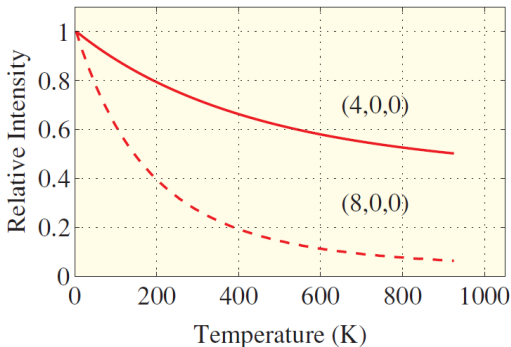
$$B_T = \frac{11492T}{A\Theta^2} \phi(\Theta/T) + \frac{2873}{A\Theta}$$

diamond is very stiff and Θ does not vary much with temperature

copper has a much lower Debye temperature and a wider variation of thermal factor with temperature

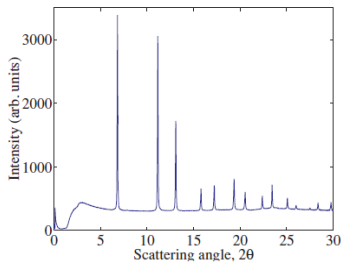
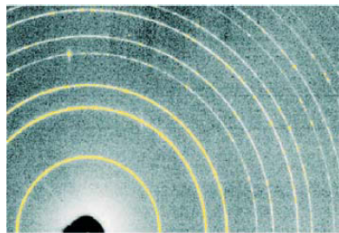
	A	Θ (K)	$B_{4.2}$	B_{77} (\AA^2)	B_{293}
C*	12	2230	0.11	0.11	0.12
Al	27	428	0.25	0.30	0.72
Cu	63.5	343	0.13	0.17	0.47

*diamond

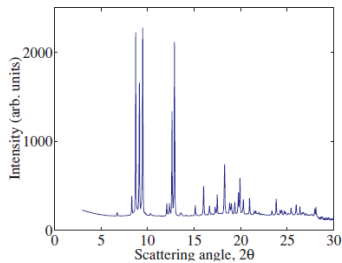


Powder diffraction

(a) Ambient pressure



(b) 4.9 GPa (49 kbar)



CaO-CaO₂ reaction kinetics

CaO is a possible material to be used for carbon sequestration

CaO-CaO₂ reaction kinetics

CaO is a possible material to be used for carbon sequestration

CaO will absorb CO₂ at temperatures as low as 450°C forming CaCO₃ and can be regenerated by calcination at temperatures above 700°C

CaO-CaO₂ reaction kinetics

CaO is a possible material to be used for carbon sequestration

CaO will absorb CO₂ at temperatures as low as 450°C forming CaCO₃ and can be regenerated by calcination at temperatures above 700°C

It is important to understand the fundamental reaction kinetics of these processes in order to be able to design carbon sequestration procedures.

CaO-CaO₂ reaction kinetics

CaO is a possible material to be used for carbon sequestration

CaO will absorb CO₂ at temperatures as low as 450°C forming CaCO₃ and can be regenerated by calcination at temperatures above 700°C

It is important to understand the fundamental reaction kinetics of these processes in order to be able to design carbon sequestration procedures.

Measurements heretofore have been performed in TGA systems which have fundamental mass flow limitations. These experiments were performed at Sector 17-BM of the APS. Samples were loaded in quartz capillaries and a 2D area detector was used to take snaps at up to 0.25s/frame.

CaO-CaO₂ reaction kinetics

CaO is a possible material to be used for carbon sequestration

CaO will absorb CO₂ at temperatures as low as 450°C forming CaCO₃ and can be regenerated by calcination at temperatures above 700°C

It is important to understand the fundamental reaction kinetics of these processes in order to be able to design carbon sequestration procedures.

Measurements heretofore have been performed in TGA systems which have fundamental mass flow limitations. These experiments were performed at Sector 17-BM of the APS. Samples were loaded in quartz capillaries and a 2D area detector was used to take snaps at up to 0.25s/frame.

Rietveld refinement was used to measure the lattice parameters, crystallite sizes and phase fractions during carbonation and calcination cycles

CaO-CaO₂ reaction kinetics

CaO is a possible material to be used for carbon sequestration

CaO will absorb CO₂ at temperatures as low as 450°C forming CaCO₃ and can be regenerated by calcination at temperatures above 700°C

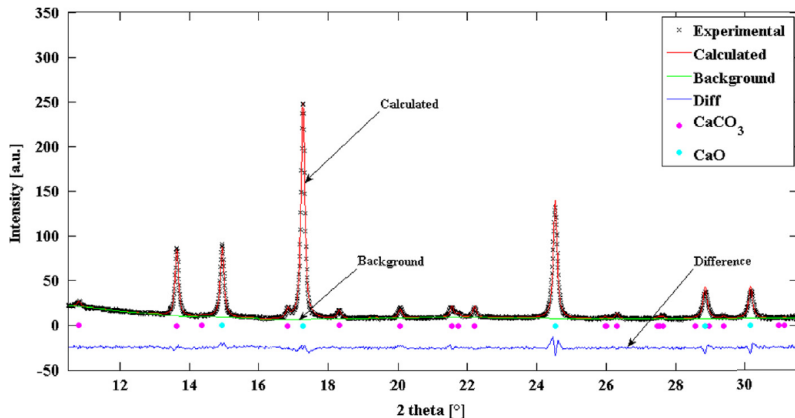
It is important to understand the fundamental reaction kinetics of these processes in order to be able to design carbon sequestration procedures.

Measurements heretofore have been performed in TGA systems which have fundamental mass flow limitations. These experiments were performed at Sector 17-BM of the APS. Samples were loaded in quartz capillaries and a 2D area detector was used to take snaps at up to 0.25s/frame.

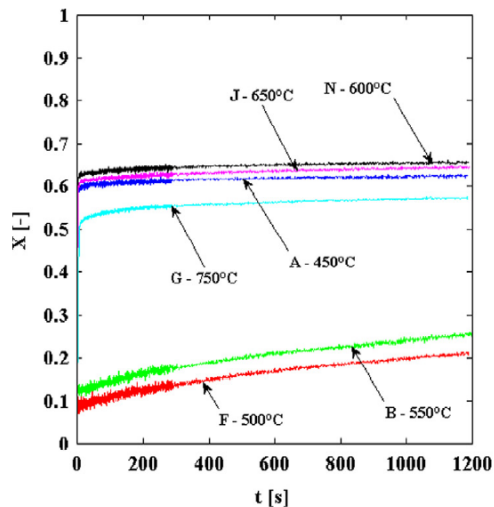
Rietveld refinement was used to measure the lattice parameters, crystallite sizes and phase fractions during carbonation and calcination cycles

A. Biasin, C.U. Segre, G. Salviulo, F. Zorzi, and M. Strumendo, *Chemical Eng. Sci.* **127**, 13-24 (2015)

CaO-CaO₂ reaction kinetics

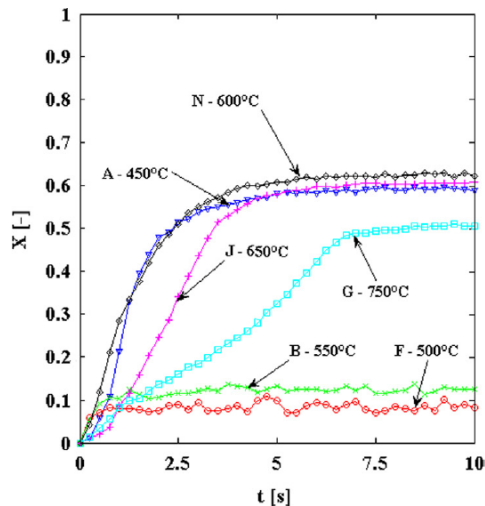


CaO-CaO₂ reaction kinetics



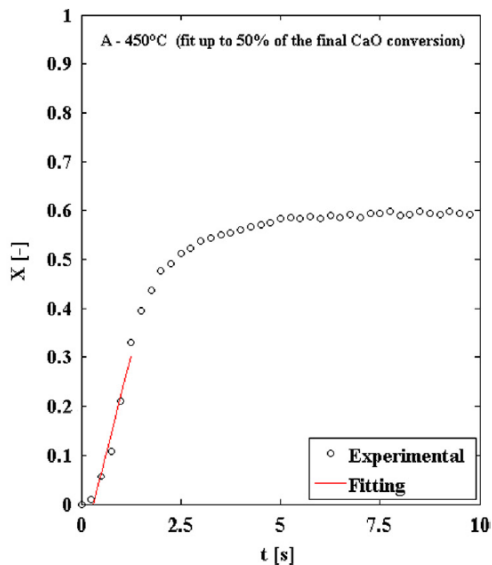
Final conversion fraction depends on temperature but also some other parameter (what?)

CaO-CaO₂ reaction kinetics

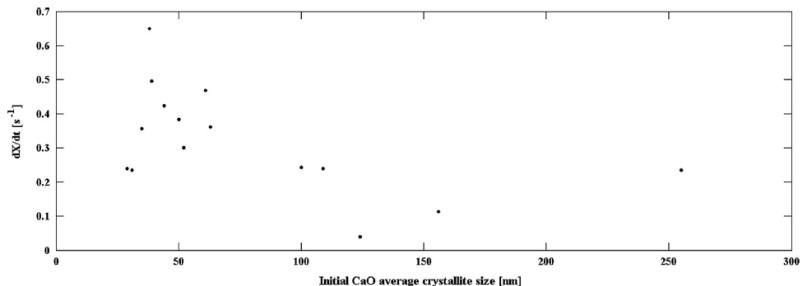


Reaction kinetics much faster than previously observed (0.28/s)

CaO-CaO₂ reaction kinetics



CaO-CaO₂ reaction kinetics



Initial crystallite size is one of the determining factors in initial rate of conversion and fraction converted.

CaO crystallite size can be related to porosity which is key to the conversion process.